Kamel Barra

J. Electrical Systems 5-1 (2009):

Regular paper

Adaptive Nonlinear Generalized Predictive Controller for Induction Motor Drives

The paper deals with the application of Direct Adaptive Nonlinear Generalized Predictive Control DANGPC method to an induction motor drive. The proposed approach is applied to overcome time-varying parameters effects namely the inertia moment and friction coefficient of the linearized speed loop and to increase the tracking performance. The used algorithm does not need the knowledge of system parameters. Simulation results demonstrate the robustness against parameter variations, and a higher dynamic behavior is obtained when compared to Nonlinear Predictive Control NGPC version.

Keywords: Induction motor, adaptive control, Nonlinear control, generalized predictive control.

1. Introduction

Induction motors are receiving wide attention in industrial applications due to their large speed capability, mechanical robustness, cheapness and ease of maintenance. They however, represent highly nonlinear, coupled, multivariable, complex control plant with unknown disturbances and time varying parameters requiring complex control algorithms. Therefore, they are more difficult to control than DC motors where torque and flux are naturally decoupled and can be controlled independently allowing fast torque response and high precision in the regulation loop [1].

The weakness of the field oriented control method is related to the exact knowledge of the reference frame (d-q) position which is not measurable and on the other hand when the motor operates in the over-speed region the decoupling becomes only partial. In order to cope with the points mentioned above, an input-output linearization control appears as a good alternative to obtain the exact decoupling torque (speed)/flux [2],[3],[4].

As stated in many previous studies on input–output decoupling and linearization [4][5][6][7], Van Raumer [5] has proposed a controller designed to track torque and rotor flux references, Marino *et al*. [7] have developed an input–output decoupling controller which decouples the regulation of rotor speed and rotor flux norm, Morever in [3][4] Maaziz has developed a nonlinear predictive control with feedback linearization to overcome nonlinear systems difficulties such as: nonlinear dynamic model and observation of rotor flux, and it was shown that the motor model used was not entirely linearizable and the largest feedback linearizable subsystem is of dimension 3 or 4 instead of 5[6][7]. Note that any of the previous studies on nonlinear predictive control has discussed the control robustness against parameters variations especially when the drive operates under a wide range of changing load charcteristics where the mechanical system parameters vary substantially due to inertia moment and friction constant.

Department of Electrical Engineering, Larbi Ben M'hidi university, Oum El Bouaghi, 04000. Algeria,
barakamel@yahoo.fr

The prediction is a concept which plays a significant role in any activity in which we seek to anticipate a trajectory such as in walk, control of a car or in a sports activity. we seeks to anticipate a trajectory in control to envisage the gestures and operations to be carried out. It is on this intuitive concept and naturalness that is based the predictive control [3],[8]. Over the last decades, generalized predictive control GPC has received an increasing attention in many control applications and it has shown to be an effective strategy for good performance applications compared to some conventional control methods with good temporal and frequency properties (small overshoot, cancellation of disturbances, good stability and robustness margins)[4]. GPC is a model based method which employs receding horizon approach in order to predict future outputs. An appropriate sequence of the control signalsis then calculated to reduce the tracking error by minimizing a quadratic cost function [4].

The adjunction of an adaptive loop to the predictive tracking velocity loop gives more performances to the control system. Indeed, the main loop ensures the tracking of the reference signal by using a nonlinear "fixed" GPC controller, and then the secondary loop is directly related to parameters variation and gives the adaptive effect [10][11].

In this paper, an adaptive nonlinear predictive controller has been proposed in order to reduce the performance degradation due to mechanical time constant variation. The DANGPC control does not need knowledge of the motor parameters, since it compares the actual behaviour with the predicted one and the parameters are adapted consequently at each sampling period giving the optimal command on-line. The algorithm uses a recursive least squares RLS and gradient type strategies for the parameters on-line identification.

The extensive simulation computer demonstrates, when compared with the classical "fixed" nonlinear predictive controller NGPC the best performances of the DANGPC controllers against time-varying parameters.

2. Nonlinear induction motor model

A squirrel cage induction motor model used under simplified assumptions where iron saturation, skin effect, heating variations of stator and rotor resistances are neglected. The model can be expressed by the fifth-order model in the stator fixed *(α-β)* frame as follows [é][4]:

$$\dot{x} = f(x) + gu \tag{1}$$

where:

$$f(x) = \begin{bmatrix} -\gamma i_{s\alpha} + \dfrac{K}{T_r}\phi_{r\alpha} + p\Omega K\phi_{r\beta} \\ -\gamma i_{s\beta} - p\Omega K\phi_{r\alpha} + \dfrac{K}{T_r}\phi_{r\beta} \\ \dfrac{L_m}{T_r} i_{s\alpha} - \dfrac{1}{T_r}\phi_{r\alpha} - p\Omega\phi_{r\beta} \\ \dfrac{L_m}{T_r} i_{s\beta} + p\Omega\phi_{r\alpha} - \dfrac{1}{T_r}\phi_{r\beta} \\ p\dfrac{L_m}{JL_r}(\phi_{r\alpha} i_{s\beta} - \phi_{r\beta} i_{s\alpha}) - \dfrac{(f\Omega + C_r)}{J} \end{bmatrix} \tag{2}$$

$$
\begin{aligned}
x &= \left[i_{s\alpha}, i_{s\beta}, \phi_{r\alpha}, \phi_{r\beta}, \Omega\right]^T \\
u &= \left[u_{s\alpha}, u_{s\beta}\right]^T \\
g &= \begin{pmatrix} \frac{1}{\sigma L_s} & 0 & 0 & 0 & 0 \\ 0 & \frac{1}{\sigma L_s} & 0 & 0 & 0 \end{pmatrix}^T \\
K &= \frac{L_m}{\sigma L_s L_r}; \quad \sigma = 1 - \frac{L_m^{\,2}}{L_s L_r} \quad \gamma = \frac{R_s}{\sigma L_s} + \frac{R_r L_m^{\,2}}{\sigma L_s L_r^2}
\end{aligned}
\tag{3}
$$

$i_{s\alpha}$, $i_{s\beta}$: denote the stator currents,
$\phi_{r\alpha}, \phi_{r\beta}$: the rotor fluxes,
$u_{s\alpha}, u_{s\beta}$: the stator voltage, The motor is fed by a voltage inverter.
R_s, R_r, L_s, L_r : the stator and rotor resistances and inductances.
$T_r = \frac{L_r}{R_r}$: rotor constant time.
p: Number of pole pairs

Considering the mechanical speed Ω and rotor flux modulus as outputs, with y_1 as the speed and y_2 as the rotor flux norm:

$$
y = \begin{pmatrix} y_1 = \Omega \\ y_2 = \sqrt{\phi_{r\alpha}^2 + \phi_{r\beta}^2} = \phi_r \end{pmatrix}
\tag{4}
$$

With the previous assumptions, a non entierly linearisable state space model is derived with five state variables ($i_{s\alpha}, i_{s\beta}, \phi_{r\alpha}, \phi_{r\beta}, \Omega$) because all state variables and commands ($u_{s\alpha}, u_{s\beta}$) can be expressed as a finite number of outputs (Ω, ϕ_r), their time derivatives and their first integrals so that [4]:

- If the rotor flux ϕ_r is written under its complex form $\bar{\phi}_r = \phi_r \, e^{j\rho}$ where ϕ_r is the rotor flux amplitude and ρ the argument, one can deduce that:

$$
\begin{aligned}
\bar{\phi}_r &= \phi_r \exp\left(j \frac{R_r}{p} \int_0^t \left(\frac{J\dot{\Omega}}{\phi_r^2} + \frac{f\Omega}{\phi_r^2} + \frac{C_r}{\phi_r^{\,2}} \right) dt \right) \\
\bar{\phi}_r &= A\left(y_2, \int y_1, \int (\dot{y}_1, y_2)\right)
\end{aligned}
\tag{5}
$$

- Stator current can be expressed as:

$$
\begin{aligned}
\bar{i}_s &= \frac{1}{L_m} e^{jp\theta} \left(\phi_r e^{j\rho} + \frac{L_r}{R_r} \left(\dot{\phi}_r + j \frac{R_r}{p} \left(\frac{J\dot{\Omega}}{\phi_r^{\,2}} + \frac{f\Omega}{\phi_r^{\,2}} \right) \right) e^{j\rho} \right) \\
\bar{i}_s &= B\left(y, \dot{y}, \int y, \int \dot{y}\right)
\end{aligned}
\tag{6}
$$

- Stator voltage (command) can be also derived as:

$$\bar{u}_s = u_{s\alpha} + ju_{s\beta} = R_s \bar{i}_s + \frac{d\bar{\phi}_s}{dt}$$

$$\bar{u}_s = \left(\frac{R_s}{L_m} \left(\phi_r + T_r \left(\dot{\phi}_r + j\dot{\rho}\phi_r \right) \right) e^{j\rho} + \right.$$

$$\left. \frac{d}{dt} \left\{ \left(\frac{L_s}{L_m} \phi_r + \frac{L_s L_r - L_m^2}{L_m R_r} \left(\dot{\phi}_r + j\dot{\rho}\phi_r \right) \right) e^{j\rho} \right\} e^{jp\theta} \right. \tag{7}$$

$$\bar{u}_s = C\left(y, \dot{y}, \ddot{y}, \int y, \int \dot{y} \right)$$

By denoting :

$$e^{j(p\theta+\rho)} = e^{j\delta} = \cos\delta + j\sin\delta \tag{8}$$

One can get the stator voltage components as the open loop commands of the nonlinear system:

$$\bar{u}_s = u_{s\alpha} + ju_{s\beta} = f_{NL1} + jF_{NL2}$$

$$u_{s\alpha} = \frac{R_s}{L_m} \left(\phi_r \cos\delta + T_r \dot{\phi}_r \cos\delta - T_r \phi_r \dot{\rho} \sin\delta \right)$$

$$+ \frac{L_s}{L_m} \left(\dot{\phi}_r \cos\delta - \phi_r \dot{\delta} \sin\delta \right) + \frac{L_s L_r - L_m^2}{L_m R_r} x \tag{9}$$

$$\left(\ddot{\phi}_r \cos\delta - \phi_r \dot{\rho}\dot{\delta} \cos\delta - \phi_r \ddot{\rho} \sin\delta - \dot{\phi}_r \dot{\delta} \sin\delta \right)$$

$$u_{s\beta} = \frac{R_s}{L_m} \left(\phi_r \sin\delta + T_r \dot{\phi}_r \sin\delta + T_r \phi_r \dot{\rho} \cos\delta \right) +$$

$$\frac{L_s}{L_m} \left(\dot{\phi}_r \sin\delta + \phi_r \dot{\delta} \cos\delta \right) + \frac{L_s L_r - L_m^2}{L_m R_r} x \tag{10}$$

$$\left(\ddot{\phi}_r \sin\delta - \phi_r \dot{\rho}\dot{\delta} \sin\delta + \phi_r \ddot{\rho} \cos\delta + \dot{\phi}_r \dot{\delta} \cos\delta \right)$$

The open loop planified rotor flux argument can be derived as:

$$\dot{\rho} = \frac{R_r}{p\phi_r^2} \left(J\dot{\Omega} + f\Omega \right) = \frac{R_r}{p\phi_r^2} . C_{emrefOL} \tag{11}$$

Where :

$$\dot{\delta} = \dot{\rho} + p\dot{\theta} = \dot{\rho} + p\Omega \tag{12}$$

The term $\left(J\dot{\Omega} + f\Omega \right)$ in (11) corresponds to reference torque of nonlinear voltage control. Nevertheless, this model can be used as reference model in predictive control (GPC/MRM version) to improve dynamic performances of the system controlled in closed loop.

Now, by using a diffeomorphism, it is possible to obtain a state feedback which linearises and decouples the system with the speed and rotor flux norm as outputs.

Several studies [4],[5],[6],[7],[8] showed that this technique of feedback linearisation revealed interesting properties as for decoupling speed/flux loops. We define (v_1,v_2) the new entries of the Nonlinear Reference Control *N.L.R.C.* and the model of the system, we

assume here that the input-output transfers (y_1,v_1) and (y_2,v_2) will enjoy the linear systems properties.

The new entries (v_1,v_2) are chosen as :

$$\begin{cases} v_1 = J\dot{\Omega} + f\Omega \\ v_2 = \ddot{\phi}_r = \ddot{y}_2 \end{cases} \tag{13}$$

Then a least squares identification is used to validate the model of the system and can be then represented by two decoupled monovariable subsystems according to fig.1.

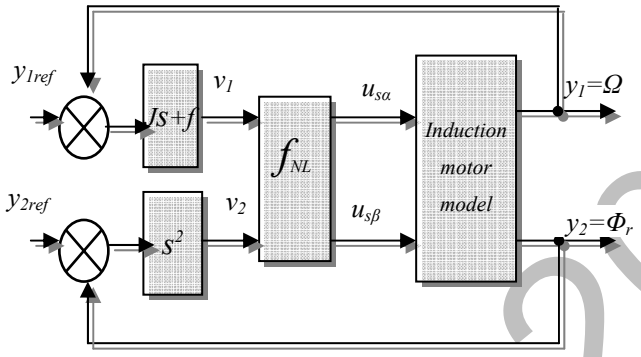

Fig. 1: Decoupled monovariable subsystems.

The reference torque in the closed loop $C_{emrefCL}$ is formed according to:

$$C_{emCL} = C_{emrefOL} + C_{CLy1} \tag{14}$$

$$C_{emrefOL} = J\dot{y}_{1ref} + fy_{1ref} \tag{15}$$

where C_{CLy1} is the output of RST predictive controller superposed to the electromagnetic reference torque in the open loop $C_{emrefOL}$. Here two monovariable generalized predictive controllers GPCwith multiple reference models GPC/MRM algorithms based on a RST structure have been used for both speed and rotor flux loops according to the block diagram of fig. 3.

3. The standard Generalized Predictive Control

The GPC control law uses CARIMA representation:

$$A(q^{-1})y(t) = q^{-1}B(q^{-1})u(t) + \frac{\xi(t)}{\Delta(q^{-1})} \tag{16}$$

Where *u(t)* and *y(t)* are the plant input and output for a SISO system. *A* and *B* are polynomials in the backward shift operator q^{-1} and $\Delta\left(q^{-1}\right) = 1 - q^{-1}$. $\xi(t)$ is an uncorrelated random sequence. The *j*-step ahead prediction over the costing horizons $N_1 \le j \le N_2$ is given by :

$$\hat{y}(t+j) = \underbrace{G_j(q^{-1})\Delta u(t+j-1)}_{\text{terme lié aux commandes futurs}} + \underbrace{F_j(q^{-1})y(t) + H_j(q^{-1})\Delta u(t-1)}_{\text{Réponse libre}} \tag{17}$$

where F_j , G_j , H_j are polynomials obtained by solving Diophantine equations.

To achieve optimal command values, the GPC uses a quadratic cost function defined as:

$$J_{GPC} = \sum_{j=N_1}^{N_2} \left[w(t+j) - \hat{y}(t+j) \right]^2 + \lambda \sum_{j=N_1}^{N_u} \left[\Delta u(t+j-1) \right]^2 \tag{18}$$

The matrix form of the predictor (8):

$$\hat{Y} = \boldsymbol{G}\,\tilde{U} + \boldsymbol{F}\; y(t) + \boldsymbol{H}\;\Delta u(t-1) \tag{19}$$

Minimisation of (9) gives the optimal control values, only the first value is applied on the system

$$\tilde{U}_{opt} = M\,(W - \mathrm{F})$$

$$M = \left[\boldsymbol{G}^T\,\boldsymbol{G} + \lambda\; I_{N_u} \right]^{-1}\; \boldsymbol{G}^T = \begin{pmatrix} M_1 \\ \vdots \\ M_{N_u} \end{pmatrix} \tag{20}$$

Where :

$$\tilde{U} = [\Delta u(t)\ ,\ .....,\ \Delta u(t+N_u-1)]^T$$

$$\hat{Y} = [\hat{y}(t+N_1)\ ,.....,\ \hat{y}(t+N_2)]^T$$

$$W = [w(t+N_1)\ ,.....,\ w(t+N_2)]^T$$

The polynomials R-S-T can be identified by:

$$\begin{cases} S\left(q^{-1}\right) = \left(1 + M_1\,\boldsymbol{H}\;q^{-1}\right) \ , & \text{degré}\left[S\left(q^{-1}\right)\right] = \text{degré}\left[B\left(q^{-1}\right)\right] \\ R\left(q^{-1}\right) = M_1\,\boldsymbol{F} \quad , & \text{degré}\left[R\left(q^{-1}\right)\right] = \text{degré}\left[A\left(q^{-1}\right)\right] \\ T\left(q^{-1}\right) = M_1\left[q^{N_1}\ \ \ldots\ q^{N_2}\right] \end{cases} \tag{21}$$

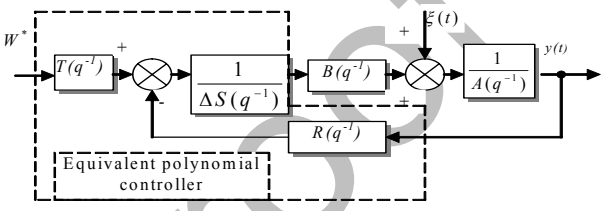

Fig. 2 : GPC Equivalent polynomial RST controller

Note that the polynomial form RST for GPC controllers is adopted to minimize on line calculations.

The GPC/MRM with multiple reference models imposes that the predicted output follows a reference trajectory y_r obtained via a filtered setpoint W coupled to a reference control trajectory signal u_r so that the quadratic cost function of (18) is now modified as:

$$J = \sum_{j=N_1}^{N_2} \left(\hat{y}(t+j) - y_{ref}(t+j) \right)^2 + \lambda \sum_{j=1}^{N_u} \left(\Delta u(t+j-1) - \Delta u_{ref}(t+j-1) \right)^2 \tag{22}$$

Assuming that: $\Delta u(t+j-1) = \Delta u_{ref}(t+j-1)$ for $j \geq N_u$

Minimisation of this cost function for both speed loop and rotor flux loop provides the control law to apply to the system:

- speed loop :

$$u_1(t) = u_{r1}(t) + \frac{R_1(q^{-1})}{\Delta S_1(q^{-1})} \left(y_{r1}(t) - y_1(t) \right) \tag{23}$$

- Flux loop

$$u_2(t) = u_{r2}(t) + \frac{R_2(q^{-1})}{\Delta S_2(q^{-1})}\left(y_{r2}(t) - y_2(t)\right) \quad (24)$$

The electromagnetic torque in closed loop is now obtained by superposing its value in the open loop (planified reference torque) to the control signal issued from RST controller according to relation (23).

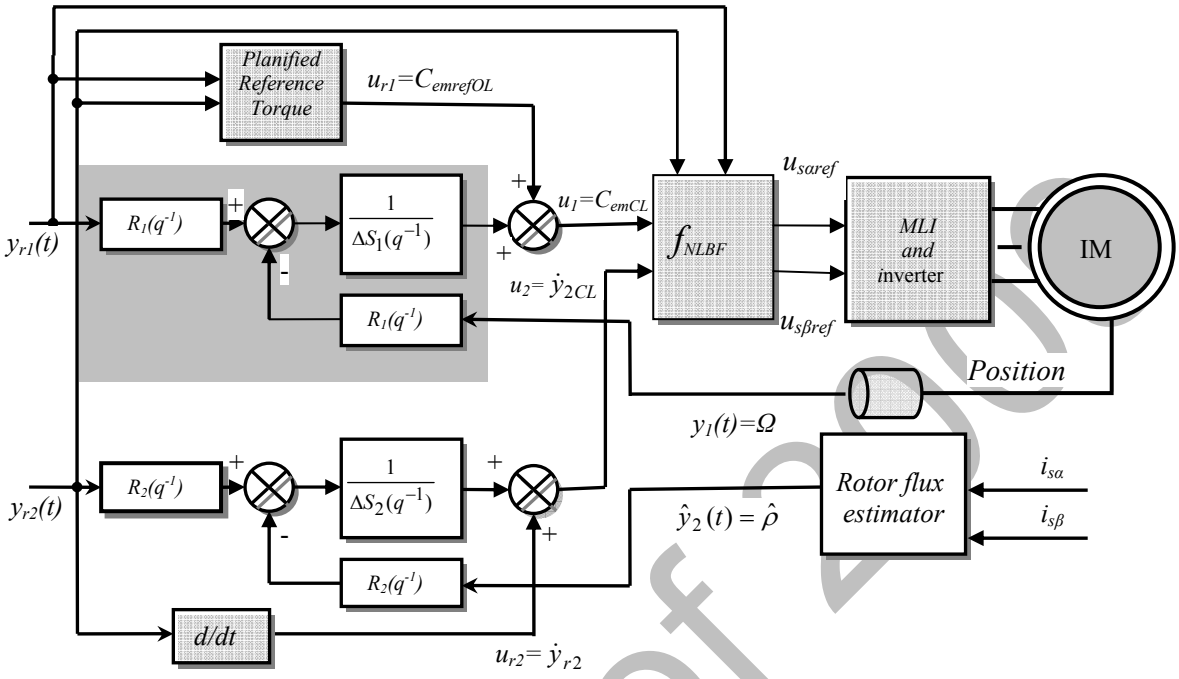

Fig. 3: Configuration of the control system

4. Simulation results

The reference trajectories for both speed and rotor flux are obtianed through the setpoints (tracking model). The command profile is chosen as a trapezoidal form for speed and as a nominal constant value for rotor flux, both filtered by a second order filter ($\omega_0 = 50rd/s, \xi = 1$)). The unloaded motor used here is the same one given in [3]:

$R_s = 8\ \Omega,\ R_r = 3.6\ \Omega,\ L_s = 0.47$ H, $L_r = 0.47$ H, $L_m = 0.452$ H, $p = 2$,

$J = 0.015$ Kg.m^2, $f = 0.01$ N.m.s^{-1} $\phi_{rn} = 1.14$ Wb , $C_{nom} = 5$ Nm.

The GPC parameters have been chosen to design robust controllers as shown in table 1

	N_1	N_2	N_u	λ
Speed loop	1	25	1	0.0115
Flux loop	1	20	1	98.222

Table 1: Tuning parameters for speed and rotor flux loops.

We assume here that the flux is measurable and the two loops models are described by discretisation of their transfer fuctions obtained after linearisation.

The first set of simulation results is obtained in the nominal parameters case where speed motor, rotor flux norm, motor torque, stator current and stator voltage are illustrated by the following figures (4)-(12)

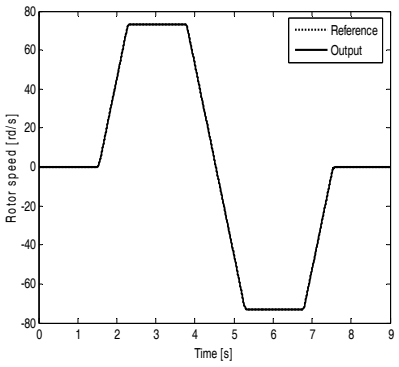

Fig. 4 : Reference speed speed motor

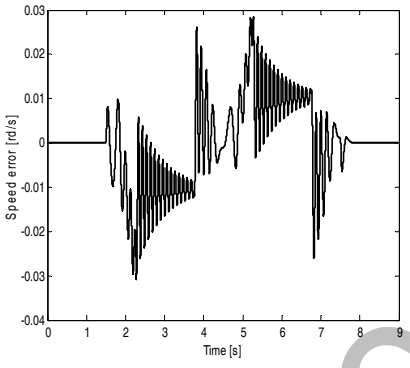

Fig. 5 : Speed error

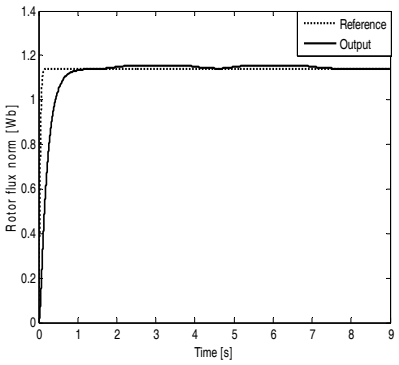

Fig. 6 : Reference flux and rotor flux norm

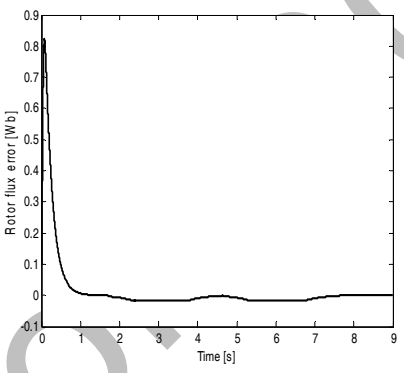

Fig. 7 : Flux error

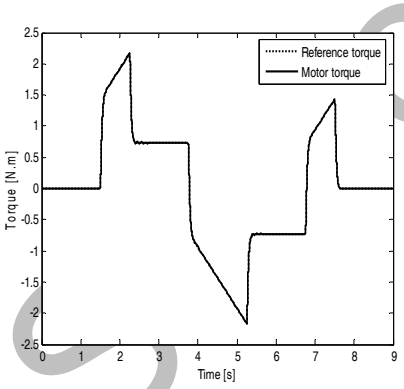

Fig. 8 : Reference torque and electromagnetic torque

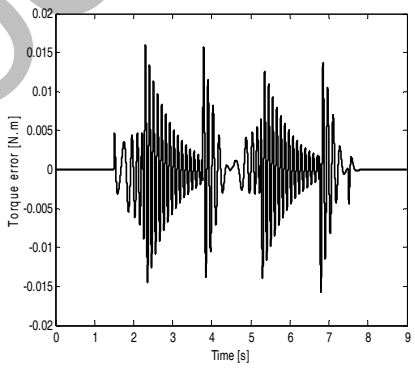

Fig. 9 : Torque error

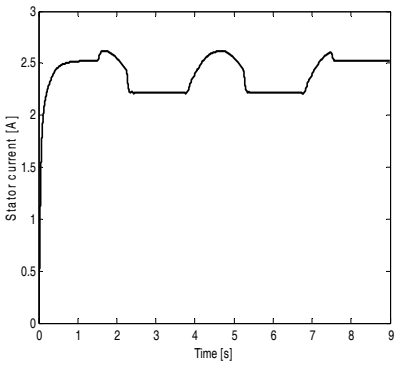

Fig. 10 : Stator current

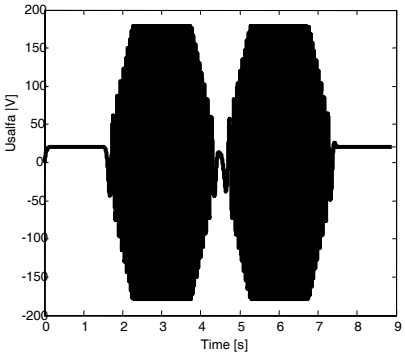

Fig. 11 : Usalfa voltage

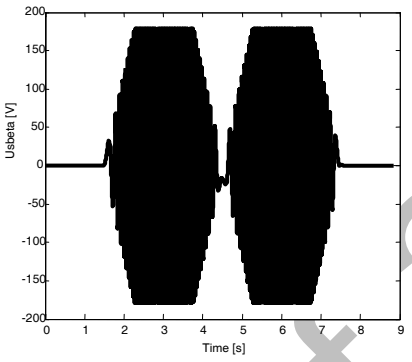

Fig. 12 : Usbeta voltage

As can be seen, the good tracking performances between outputs and their reference values for speed and flux is evident, also the electromagnetic torque is very close to the planified reference torque in an open loop strategy. Figures (10),(11),(12) depicts the stator current variations of the unloaded motor and the admissible stator voltage.

In [4], the robustness of the nonlinear control law NGPC was investigated against stator and rotor resistances and inductances variations. Here we examine a mismatched case which corresponds to variations of inertia momernt and friction coefficient.

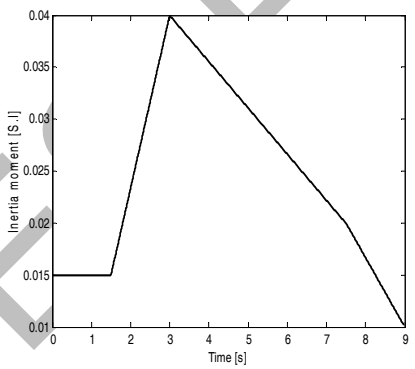

Fig. 13: Inertia moment variations

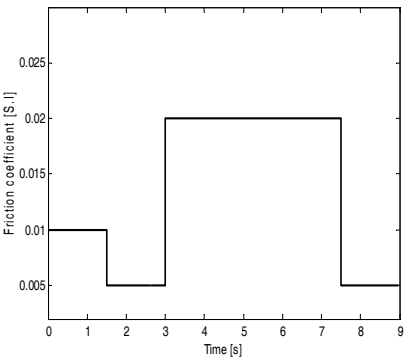

Fig. 14 : Friction variations

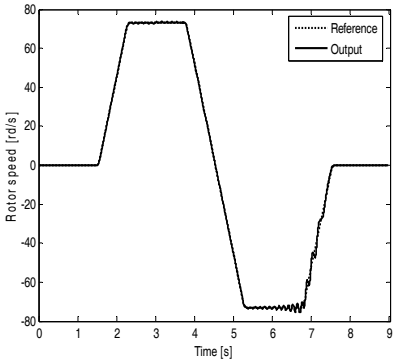

Fig. 15 : Speed profile

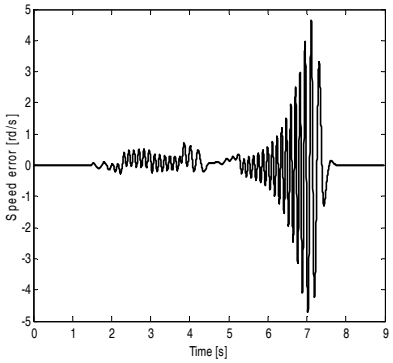

Fig. 16 : Speed error

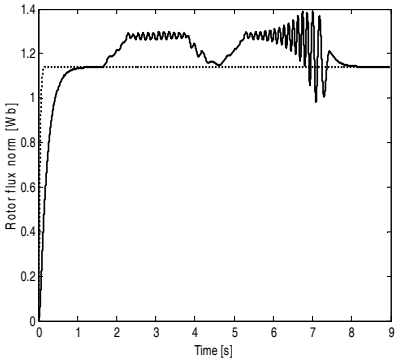

Fig. 17 : Rotor flux norm

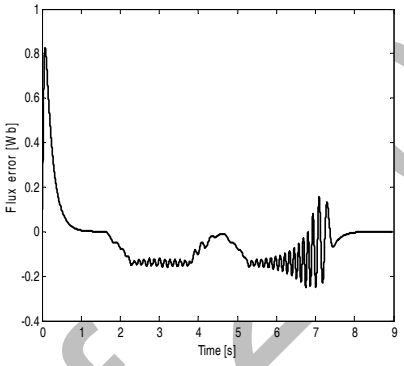

Fig. 18 : Flux error

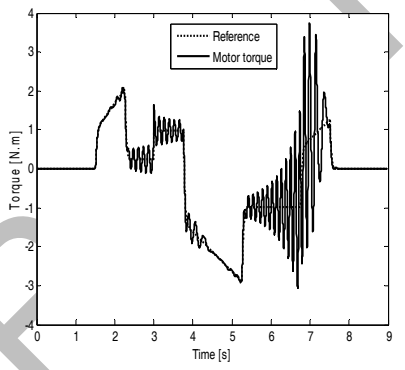

Fig. 19 : Motor torque and its reference.

The nonlinear predictive controllers are tested in the presence of mechanical parameters variations (*J* and *f* are respectively inertia moment and friction coefficient) by considering extreme and substantially variations as it is illustrated by figures (13-14). The behavior of the drive system performances in the mismatched case is poor generating sluggish and oscillatory torque and flux norm as it can be seen in figures (17) and (19). Note that the sampling period is choosen equal to 0.0001s.

To cope with these problems, it is necessary to adjunct to the nonlinear predictive control mentioned above an adaptive structure which corresponds in this study to a direct adaptive control applied to the speed loop (grey area of the figure 3) where mechanical parameters have a significant effect. The main loop (regulation loop) ensures the tracking

of the reference signal by using a nonlinear "fixed" GPC controller, and then the secondary loop (adaptive loop) is directly related to parameters variation and gives the adaptive effect.

5. Adaptive GPC

By expressing the quantity (*MW*) of the equation (20) in the form of scalar product of parameters vector $\theta(t)$ and a regressor vector containing available measurements on both output and input to the considered moment $\phi(t)$, with [11]:

$$\begin{aligned} MW &= \tilde{U} + M\,\boldsymbol{F}\,y(t) + M\,\boldsymbol{H}\,\Delta u(t-1) \\ MW &= \theta^T \phi(t) \end{aligned} \tag{25}$$

$$\begin{aligned} \phi(t) &= \left[y(t)\ \ldots\ y(t-n_a)\ \tilde{U}^T\ \Delta u(t-1)\ \ldots \Delta u(t\text{-}n_b)\right]^T \\ \theta^T &= \left[M\boldsymbol{F}\ \ \boldsymbol{I}_{nu}\ M\boldsymbol{H}\right] \end{aligned} \tag{26}$$

It is noticed that the first line of the matrix parameters $\theta(t)$ of the relation (25) is only the coefficients of the polynomials $R = M_1\boldsymbol{F}$ and $S^* = M_1\boldsymbol{H}$

By introduction of the predicted outputs between the horizons (N_1, N_2) and future control values up to horizon N_u :

$$X(t+N_2) = \left[\hat{Y}^T\ \ \tilde{U}^T\right]^T \tag{27}$$

and the vector targets *L* of the same dimension $(N_2\text{-}N_1\text{+}N_u\text{+}1)$ by considering that the vector left must converge towards the reference vector *W* and that the control signal $\tilde{U}$ made of the increments must converge towards zero:

$$L(t+N_2) = \left[W^T\ \ 0\right]^T \tag{28}$$

Thus one can define the target error as:

$$e_c(t+N_2) = X(t+N_2) - L(t+N_2) \tag{29}$$

The performance error e_p is defined by using a weighting matrix *P* of dimensions $(N_2\text{-}N_1\text{+}N_u\text{+}1)$ x N_u on the target error in order to create a cancellation dynamics of the error e_c:

$$\begin{aligned} e_p &= P^T\left[e_c(t+N_2)\right] = P^T\left[X(t+N_2) - L(t+N_2)\right] \\ &= K(t+N_2) - K_1(t+N_2) \end{aligned} \tag{30}$$

Here, *K* is an indication of the measured performances and K_1 is an evalution of the expected performances, where:

$$\begin{aligned} K(t+N_2) &= \left[M\quad \lambda Q\right]\begin{bmatrix}\hat{Y}\\ \tilde{U}\end{bmatrix} = M\hat{Y} + \lambda Q\tilde{U} \\ K_1(t+N_2) &= \left[M\quad \lambda Q\right]\begin{bmatrix}W\\ 0\end{bmatrix} = MW \\ P^T &= \left[M\quad \lambda Q\right] \\ Q &= \left[\boldsymbol{G}^T\boldsymbol{G} + \lambda I_{N_u}\right]^{-1},\ M = Q\boldsymbol{G}^T \end{aligned} \tag{31}$$

When the parameters are time-varying, the indicator of measured performances is different from that of the expected performances and when the parameters are constant the two indices coïncidents since the performances are maintained and the target error is zero. The expected performance of the process must equalizes at every moment with the initial one:

$$K_1(t+N_2) = MW = \theta^T \phi(t) \tag{32}$$

The objective in the adaptive control is to minimize the performance error at each step, that is to say thus to reach [10][11]:

$$\lim_{t \to +\infty} e_p(t) = 0 \tag{33}$$

$$e_p(t) = X(t) - \hat{\theta}(t-1)^T \phi(t-N_2)$$

The performance index to be minimized now is :

$$\begin{aligned} \Im(t+N_2) &= e_p(t+N_2)^T e_p(t+N_2) \\ &= [X(t+N_2) - L(t+N_2)]^T [X(t+N_2) - L(t+N_2)] \end{aligned} \tag{34}$$

According to the preceding relations, a diagram of adaptive predictive controller DAGPC under R-S-T form is deduced according to fig. 20.

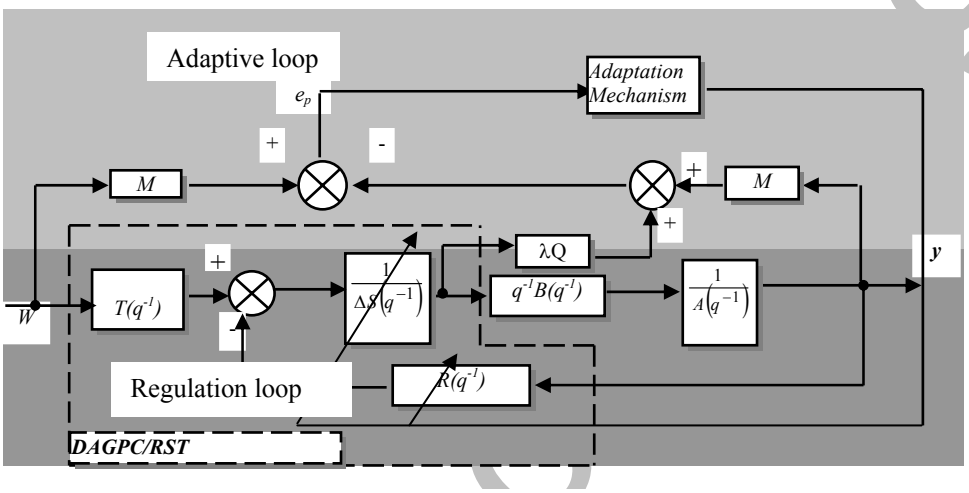

Fig. 20 : Direct adaptive GPC structure under R-S-T form

6. Configuration system

The design of direct adaptive predictive controller is recapitulated by the following steps :

1- Synthesis of the fixed predictive controller under *R-S-T* form by choosing the set of parameters stabilizing the regulation system around the nominal point.

2- Measure of the output *y*(t) and calculation of the measured performances:

$$K(t) = \begin{bmatrix} M & \lambda Q \end{bmatrix} \begin{bmatrix} \hat{Y} \\ \tilde{U} \end{bmatrix} = M\hat{Y} + \lambda Q \tilde{U} \tag{35}$$

3- Computation of the performance error:

$$e_p(t) = K(t) - \hat{\theta}(t-1)^T \phi(t-N_2) \tag{36}$$

4- Computation of the controller parameters vector:

$$\hat{\theta}(t+N_2)=\hat{\theta}(t+N_2-1)+\Gamma(t)\,\phi(t)\;\;e_p(t+N_2) \tag{37}$$

$$\Gamma(t+N_2)=\Gamma(t)-\frac{\Gamma(t)\,\phi(t)\,\phi(t)^T\,\Gamma(t)}{1+\phi(t)^T\,\Gamma(t)\,\phi(t)}$$

5- Controller parameters vector updating.

6- Application of the control value *u(t):*

$$\Delta u(t)=T(q^{-1})\,w(t)-R(q^{-1})\,y(t)-S^{*}(q^{-1})\,\Delta u(t-1) \tag{38}$$

7. Application to mechanical time constant

In the next set of simulation results, The sampling period is modified in order to sensitive the transfer function of the speed loop to parametres variations (*Te = 2 ms*) with the following tuning: *N1=1, N2=6, Nu=1, λ=4.0119;*

Both a standard GPC (nominal) and a DANGPC controllers are tested in the presence of mechanical time constant variations ($\tau = J / f$) by considering extreme variations by steps.

The normalized value of this time-constant decreases from its nominal value τ_n to ($0.7\tau_n$) and then to ($0.45\tau_n$), then it increases to ($1.25\tau_n$) and once again to ($1.5\tau_n$) before regaining its nominal value as it is illustrated by figure (21).The set of tuning parameters are the same for the two cases. For the adaptive loop, the adaptation gain is initialized to 0.1**I.**

Figure (22) depicts the load torque solicitation applied at 0.63s and cancelled at 1.35s, whereas figure (23) gives the motor velocity for low speeds region (100rd/s) and for high speed region (200d/s) for both adaptive GPC and nominal GPC. Figure (24) iluustrate the transient response for low speed region and the impact of load torque variation, the stability against several parameters variations can be seen in figure (25) and at last the transient response for high speed region given by figure (26).

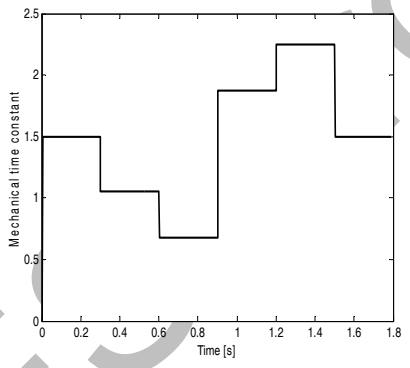

Fig. 21: Mechanical time constant variations

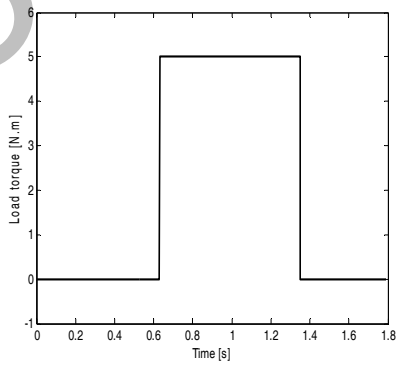

Fig. 22 : Load torque sollicitation.

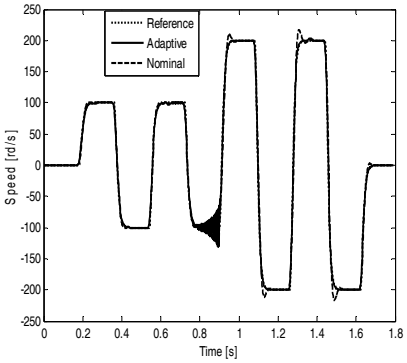

Fig. 23: Motor speed for adaptive sollicitation. and nominal GPC

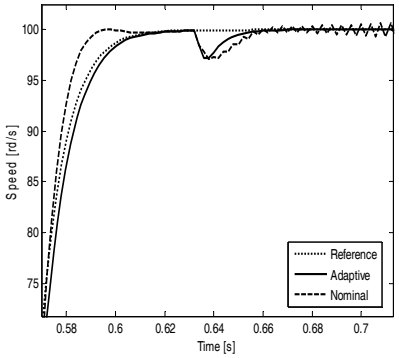

Fig. 24: Impact of load torque

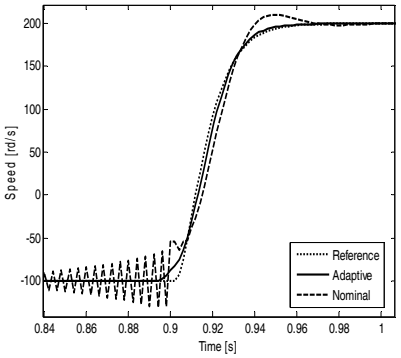

Fig. 25: Stability against several parameters variations.

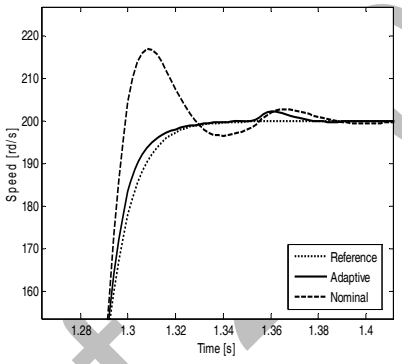

Fig.26: Transient response (Load torque cancelled at 1.35s)

The above figures (23), (24), (25), (26) display clearly the capacity of the adaptive structure to maintain a very good behavior in the presence of several parametric disturbances in term of response time, stability and overshoot. The contribution of the adaptive structure is very significant when one realizes that without the adaptive loop the motor speed becomes unstable (case of the nominal GPC given by figure (25)). Also, the disturbance rejection dynamics of the adaptive structure is better in term of amplitude and duration as it is illustarated by figures (24) and (26).

The aim of the next set of simulation results is to compare the response of the adaptive controller for both Recursive Least Squares and gradient methods. The adaptation gain is initialized to $0.1\mathbf{I}$ for RLS method and equal to $\Gamma = 0.01\mathbf{I}$ for gradient method. Note that the gradient method is very sensitive to the choice of Γ .

The algorithm of the gradient method has to minimize a quadratic criterion in term of prediction error while moving in the direction of the fastest decrease of the criterion with a constant step and causes instability if the adaptation gain is badly selected. Indeed, in the vicinity optimum, if the gain is not small it causes oscillations around the minimum. On the other hand, to have fast convergence at the beginning, the adaptation gain must have a large value.

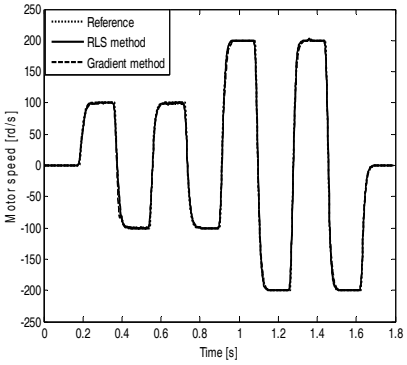

Fig. 27: Motor speed for RLS and gradient methods

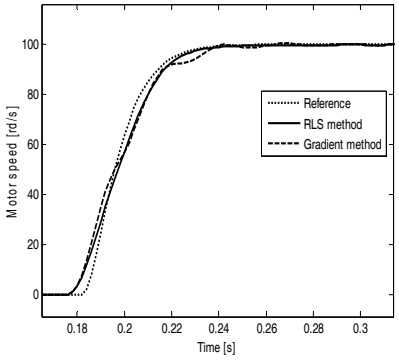

Fig. 28: Speed motor for low speed region

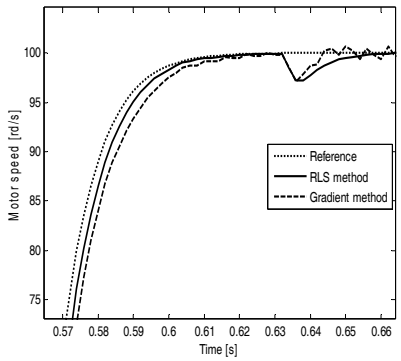

Fig. 29: Load torque impact for low speed region

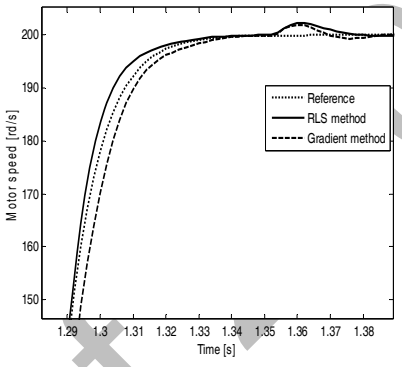

Fig. 30:Cancellation of the load torque

Figures (27),(28),(29),(30) display the superiority of the RLS method when compared to gradient method. In all cases, any adaptive method (RLS or gradient method) gets higher performances than fixed GPC in term of fast transients, stability versus parametric variations, overshoot, disturbance rejection dynamics.

8. Conclusions

The paper has presented the application of an adaptive nonlinear predictive control and feedback linearization concept to an induction motor drive. One of the results of the partially linearized control is that the transfer functions between inputs and outputs are decoupled.

Planified trajectories for speed and rotor flux in an open loop control does not allow minimization of predicted tracking errors between the output of the system and the reference. The predictive synthesis makes possible to exploit the planning of the reference signals. Indeed, simulation results show an accurate tracking of speed and flux modulus. A selective sets of simulation results have been carried out showing the high performance of the system in term of closed tracking trajectories justifying the utility of combined feedback linearisation to predictive control but not sufficiently robust against parametric variations.

To get high performances without degradation of static and dynamic response, a Direct adaptive generalized predictive controller DAGPC was adjuncted to the above control in

order to reduce the performance degradation due to mechanical parameters variations. The DANGPC control does not need knowledge of the motor parameters, since it compares the actual behavior with the predicted one and the parameters are adapted consequently at each sampling period giving the optimal command on-line.

9. References

[1] N. Golea and A. Golea, " High performance adaptive field oriented model reference control of current – fed induction motor", JEEEC journal, vol. 57, NO. 2, pp. 78-86, 2006.

[2] A. Merabet, "Commande non linéaire à modèle prédictif pour une machine asynchrone". Thèse de l'Universite du Quebec Canada 2007.

[3] M. K. Maaziz, P. Boucher and D. Dumur, "A new RST cascaded predictive control shemle for induction machines "Proc. of the 1999 IEEE ICCA conf., Hawai, USA, August 22-27-1999.

[4] M. K. Maaziz, P. Boucher and D. Dumur, "Flux and speed tracking of an induction motor based on nonlinear predictive control and feedback linearization". Proc. of the 1999 IEEE ACC conf., San Diego, USA, June 1999.

[5] T. Van Raumer and al.," Adaptive non linear speed and torque of induction machines", Proc. of the European control conference, Groningen, June 1993.

[6] Chiasson. "Dynamic feedback linearization of induction motor". IEEE trans. On Automatic control, vol. 38., n° 10, pp. 1588-1593, 1993.

[7] [12] Marino R., S. Peresada and P. Valigi, Adaptive input-output linearizing control of induction motors, IEEE Transactions on Automatic Control, vol.38, no. 2, pp. 208-221, 1993.

[8] R. Hedjar R.Toumi, P.Boucher and D. Dumur "Two cascaded nonlinear predictive controls of induction motor". IEEE 2003

[9] Boukas T.K. and T.G. Habetler, High-performance induction motor speed control using exact feedback linearization with state and state derivative feedback, IEEE Transactions on Power Electronics, vol.19, no.4, pp. 1022-1028, 2004.

[10] I. D. Landau, R. Lozano and M. M'Saad, " Adaptive control " Springer, 1997.

[11] G. Ramond, " Contribution à la commande prédictive généralisée adaptative directe et applications ", Doctorat thesis de l'école SUPELEC, France 2000.

[12] C. Pimenta and al. , "Application of direct adaptaive generalized predictive control (GPCAD) to a robotic joint", IEEE conf. on ---, 2003.

[13] M. C. Ficcara, G. Griva and F. Profumo, " Adaptive predictive speed controller for induction motor drives", IEEE conf. on --, 1999. (0-7803-5735-3/99 IEEE)